ORIGINAL ARTICLE

# Illuminating the planktonic stages of salmon lice: A unique fluorescence signal for rapid identification of a rare copepod in zooplankton assemblages

Cameron R. S. Thompson[1] | James E. Bron[2] | Samantha Bui[3] |
Sussie Dalvin[1] | Mark J. Fordyce[4] | Tomasz Furmanek[1] | Gunnvør á Norði[5] |
Rasmus Skern-Mauritzen[1]

[1]Institute of Marine Research, Bergen, Norway

[2]University of Stirling, Stirling, Scotland

[3]Institute of Marine Research, Matre, Norway

[4]Marine Scotland Science, Aberdeen, Scotland

[5]Fiskaaling - Aquaculture Research Station of the Faroes, Hvalvík, Faroe Islands

**Correspondence**
Cameron R. S. Thompson, Institute of Marine Research, Bergen N-5817, Norway.
Email: Cameron.thompson@hi.no

## Abstract

Monitoring of planktonic salmon louse (*Lepeophtheirus salmonis salmonis*) abundance and parameterization of key life-history traits has been hindered by labour-intensive and error-prone quantification using traditional light microscopy. Fluorescence illumination has been proposed as a means of improving visualization, but prior to this study adequate investigation of the relevant fluorescence profiles and measurement conditions has not been undertaken. We investigated the fluorescence profiles of *L. salmonis* and non-target copepod spp. with excitation and emission matrices (200–600 nm) and identified unique fluorescence signals. Fluorescence microscopy using excitation wavelengths of $470 \pm 40$ nm, and emission wavelengths of $525 \pm 50$ nm, showed that after 90 days of formalin storage salmon lice have a mean fluorescence intensity that is 2.4 times greater than non-target copepods (copepodid and adult stages). A 7-day heat treatment of 42°C in formalin increased the difference between salmon louse copepodids and non-target copepods to a factor of 3.6, eliminating the need for prolonged storage. Differences in the fluorescence signal and endogenous fluorophores were investigated with respect to variation in sea lice species, age, stage and host fish origin. Under the conditions outlined in this paper, the fluorescence signal was found to be a reliable means of visualizing and differentiating salmon lice from non-target zooplankters. Adaptation of the fluorescence signal would greatly expedite traditional methods of enumerating salmon louse larvae in plankton samples and could provide a means of automated detection.

**KEYWORDS**
aquaculture, Atlantic salmon, caligidae, excitation and emission matrix, *Lepeophtheirus salmonis*

# 1 | INTRODUCTION

The salmon louse, *Lepeophtheirus salmonis salmonis* (Krøyer 1837; Skern-Mauritzen et al., 2014), is an obligate ectoparasite of salmonids and a major constraint to Atlantic salmon (*Salmo salar*) aquaculture. Salmon aquaculture has expanded rapidly from a few thousand tonnes of fish produced in 1980 to the 2.4 million tonnes produced in 2018 (FAO, 2020). Norway is currently the largest producer of salmon at 1.28 million tonnes produced in 2018 (FAO, 2020), but due to environmental challenges, principally infestation by *L. salmonis*, growth of the industry has stagnated since 2012 while costs continue to rise (Bjørndal & Tusvik, 2019). Estimates of the economic impact of *L. salmonis* range from 6.2% to 8.7% of productive value (Abolofia et al., 2017; Costello, 2009a), suggesting the losses for the global salmon farming industry to be in excess of $1.26 billion USD.

Parasitic stages of *L. salmonis* feed on the mucus, tissue and blood of their host causing sores, immunosuppression and reduced feed conversion efficiency (Thorstad et al., 2015). In Norwegian waters, wild Atlantic salmon smolt migrating from rivers towards the sea are infected by *L. salmonis* copepodids suggested to primarily derive from infested farms (Fjørtoft et al., 2019; Kristoffersen et al., 2018), and the resulting lice loads increase their risk of mortality (Taranger et al., 2014). The growth of salmon aquaculture and resulting rise in *L. salmonis* infestations have been associated with declines of some wild salmonid populations, which together with welfare concerns have prompted regulatory action (Costello, 2009b; Heuch et al., 2005; Krkosek et al., 2007; Krkošek et al., 2005, 2013; Thorstad et al., 2015; Torrissen et al., 2013; Vollset et al., 2018).

The traffic light system implemented by the Norwegian government in 2017 codifies the importance of *L. salmonis* to regulatory decisions, by linking salmon aquaculture production to the risk of infestation-induced mortality in wild salmonid populations (Vollset et al., 2018). A key component of the risk assessment is the operational salmon lice model, which calculates the infection pressure through the coupling of a hydrodynamic model with a salmon lice particle tracking model. The particle model incorporates knowledge of *L. salmonis* biology and behaviour, such as development and vertical position, while the hydrodynamic model forecasts the distribution and abundance of those larval particles originating from salmon farms (Myksvoll et al., 2018, 2020; Sandvik et al., 2020). Ostensibly the operational salmon lice model describes the density of infectious copepodids, but the model output is not validated with data on planktonic stages. Rather, model validation relies on data from observation of infection pressure on wild-caught salmonids and sentinel cages (Myksvoll et al., 2018; Sandvik et al., 2016). The output of the operational lice dispersal model compares well with observed infection pressure, provides better coverage than reliance on observations alone and continues to be improved with updated information on *L. salmonis* biology (Myksvoll et al., 2018; Sandvik et al., 2016, 2020). Nevertheless, distribution and abundance of *L. salmonis* planktonic stages remain a source of uncertainty in the model, and key aspects of their biology in the planktonic stages, such as mortality, fecundity

and fine scale distribution in the field, remain underparameterized (Brooker et al., 2018; Nelson et al., 2017; Skarðhamar et al., 2019).

*Lepeophtheirus salmonis* hatch from eggs strings carried by females and develop through three non-feeding planktonic stages: nauplius 1 and 2 (N1 and N2), and the infective copepodid stage. After the copepodid finds and attaches to a host, it develops through 5 more stages concluding with the adult stage (Hamre et al., 2013). While the parasitic stages can be readily observed and enumerated on the host fish, the free-living planktonic stages can only be identified within a zooplankton sample. However, finding and enumerating planktonic *L. salmonis* are challenging due to their relative low abundance in comparison with other species typically collected in a sample. Previous studies suggest a mean abundance of planktonic stages ranging from 0.075 to 0.70 m$^{-3}$ with numerous zero counts and a few outliers, which indicates a high degree of patchiness (á Norði et al., 2015; Byrne et al., 2018; Nelson et al., 2017; Nilsen, 2016; Penston et al., 2011; Salama et al., 2013; Skarðhamar et al., 2019). In comparison, the global mean density of copepods is estimated to be 1,000 m$^{-3}$ (Box hall, 1998), and a planktonic tow from the west coast of Norway typically yields 5,000 m$^{-3}$ or more animals (T. Falkenhaug, personal communication, 6 June 2020). Thus, one may have to sort through 1,400 to 66,000 animals before identifying a single *L. salmonis* in a plankton sample.

Since identifying and enumerating planktonic *L. salmonis* stages in a zooplankton sample are a laborious task, several methodologies have been employed to that effect, with mixed results (Bui et al., 2020). Amongst them, fluorescence microscopy has been shown to increase the visibility of *L. salmonis* copepodids in comparison with other species (Bui et al., 2020; Fordyce, 2017). However, the reliability of the fluorescence signal has not been investigated nor has the optimal method been described in detail. Ideally, a specific combination of excitation and emission filters would result in *L. salmonis* fluorescing, while non-target animals are unaffected. In fluorescence, a molecule is exposed to an incident light and photons are absorbed by the molecule raising its energy level (excitation), but rather than returning to the ground level immediately, the molecule steps down its energy state and releases photons at a lower energy level with longer wavelengths (emission). The fluorescing molecule, the fluorophore, is characterized by its excitation spectrum, its emission spectrum, and its quantum yield or the amount of energy emitted divided by the energy absorbed. Thus, fluorescence is a predictable phenomenon that can be harnessed by spectroscopy to identify and quantify fluorophores (Lakowicz, 2013).

In a mixed solution where it is not possible to purify the fluorophores, the relative contribution of various compounds can be described by an excitation and emission matrix (EEM), in which the fluorescence intensity is recorded for each pair of excitation and emission wavelengths. EEM measurements have been used to characterize the dissolved organic matter in sea water, terrestrial water and waste water; classify phytoplankton communities; and identify the origin of food products (Coble et al., 1996; SádeCká & TóThoVá, 2007; Hudson et al., 2007; Richardson et al., 2010; Andrade-Eiroa et al., 2013; Carstea et al., 2016). In the same manner, this study classifies *L. salmonis* and

non-target copepod spp. that are commonly present in the planktonic assemblage with *L. salmonis*, according to their fluorescence profiles as observed by EEM measurements. However, fluorescence spectroscopy alone would not be a solution for enumerating *L. salmonis* within a plankton sample because their relative low abundance would not produce a detectable fluorescence signal.

A sufficiently large and consistent difference in fluorescence intensity between planktonic *L. salmonis* and non-target animals may be used as a signal for rapid identification. In the present study, we used EEM measurements to explore the fluorescence profiles of the target sea lice species and non-target copepod spp., and identified the wavelengths where the greatest contrast in the fluorescence occurred. The fluorescence intensity exhibited by the animals was then quantified at those wavelengths through fluorescence microscopy and analysed for statistical differences. The reliability of those fluorescence signals was further examined by investigating factors that might influence them, including storage time in formalin, host fish origin, copepodid age and developmental stage.

## 2 | METHODS

### 2.1 | Sea lice and non-target copepod sampling

To address the question of host fish origin, *L. salmonis* were sourced from farmed Atlantic salmon (*Salmo salar*), wild Atlantic salmon and sea trout (*Salmo trutta*). Another sea louse of significance to salmon aquaculture in the Northern Hemisphere is *Caligus elongatus*. It has the same planktonic life-history stages and appears almost identical to *L. salmonis* under the microscope (Schram, 2004). Therefore, *C. elongatus* females with egg strings were collected from wild fish along with *L. salmonis*, and additional egg strings were sourced from a laboratory culture.

Salmon lice eggs were sourced primarily from three laboratory strains of *L. salmonis*: LsGulen, LsOslo and Ls1A (Hamre et al., 2009), cultured at the Institute of Marine Research (IMR) facility in Bergen, Norway. Laboratory-cultured *C. elongatus* were provided by the University of Bergen (UIB) Sea Lice Research Center. *L. salmonis* and *C. elongatus* were also collected from wild fish trapped with fyke nets in various fjords in Western Norway during the spring 2019 and 2020. The female lice with egg strings obtained from adult wild fish were placed in a container with sea water from their collection point (minimum 0.25 L per female) and transported to the Bergen facility in a cooler. Additional *L. salmonis* eggs were provided by salmon farms located in Austevoll, Norway, and the Faroe Islands.

During the collection, host fish were fully anaesthetized with tricaine methanesulphonate (Finquel: 10 g 100 L$^{-1}$), and female sea lice with egg strings were removed with forceps. Egg strings were detached from the female louse and placed into incubation chambers where they hatched and developed through the planktonic stages. While the farm strains were hatched and incubated at the respective local institutions of Fiskaaling Aquaculture Research Station in the Faroe Islands and Austevoll Research Station (IMR), all others

were reared at the IMR Bergen facility. For all sources, the hatchery set-up followed that described by Hamre et al. (2009). In Bergen, the incubators were provided with flowing sea water with a salinity of 34.5 ppt and temperature of 9.5 ± 1°C. The water was pumped from the adjacent fjord at a depth of 120 m and passed through a sand filter and disc filter. Similarly, in Austevoll, the filtered sea water was pumped from a depth 165 m, with a salinity of 32.6 and a temperature of 8.4 ± 0.1°C. At Fiskaaling, the incubator was filled with filtered sea water having a salinity of 35.2 ppt. The sea water (~40 L) was recirculated between the incubator and a holding tank connected to a watercooler (BOYU L series water chiller), which kept the temperature at 10 ± 0.5°C.

During the hatching phase, unhatched egg strings were moved to a new incubation chamber every 24 hr, while hatched nauplii remained in the original chamber. This allowed the hatch time of lice in each chamber to be defined within a 12-hr error margin. N1 stage nauplii were sampled immediately, while N2 stage nauplii were sampled 3 days post-hatch (DPH), with young and old copepodids sampled at 6 DPH and 12 DPH, respectively. At a temperature of 9.5°C, the expected duration of naupliar stages is approximately 4 days, while the duration of the nauplius and infective copepodid stages together is 17 days (Stien et al., 2005; Samsing et al., 2016).

Egg strings were collected on 11 separate occasions from the Bergen *L. salmonis* culture between March 2019 and March 2020. Several cohorts of equivalent-aged nauplii and copepodids were sampled from each collection of egg strings and either measured immediately or fixed in either 70% saline ethanol (34 ppt) or 10% formalin buffered with 9% (w/v) sodium tetraborate. Each of the 34 *L. salmonis* cohorts from the 11 cultures was fixed and then divided into 5–7 separate glass containers to mitigate possible chamber effects.

Non-target copepod spp., for use as comparators with respect to target sea lice species, were collected with a vertical plankton net with a 0.5 m diameter frame and 140 μm mesh size. Repeated tows to a depth of 10–30 m were made from a Bergen pier on 24 June and 10 July 2019, and from a boat in Bjørnafjorden on 14 April and 19 November 2019, and 27 March 2020. The dominant non-target copepod spp. found in the tows and sorted for measurement included *Calanus finmarchicus*, *Acartia* spp., *Pseudocalanus* spp., *Temora* spp., *Oithona* spp. and *Centropages* spp. Apart from *Centropages* spp., those copepod species have been reported as occurring in high numbers in the North Sea, Norwegian Sea, Faroe Islands and Northern Norway (Falkenhaug et al., 1997; Gundersen, 1953; Nielsen & Andersen, 2002; O'Brien et al., 2013). Thus, they occur in regions where salmon farming is prevalent and are commonly found in the zooplankton assemblage along with *L. salmonis* and *C. elongatus*.

### 2.2 | Fluorescence fingerprinting, and excitation and emission matrix (EEM) measurements

Fluorescence intensity was measured with a Shimadzu RF-6000 Spectrofluorophotometer using the 3D analysis application. The

instrument has monochromatic filters for excitation and emission spectra. Sequentially changing the filter wavelengths along both spectra and measuring emitted light intensity produces a matrix of fluorescence data termed an excitation and emission matrix (EEM). The instrument was set to measure fluorescence intensity between 200 and 600 nm, with filter bandwidths of 10 nm for excitation and 5 nm for emission. Filter scan rate was set to 60,000 nm/min, sensitivity was set to low, and the data interval was set to 2 nm.

The RF-6000 was fitted with Shimadzu's Constant Temperature Single-Cell Holder with Stirrer and Starna's Type 18-F/MS/Q/10-Micro Cell Cuvette, which has a nominal volume of 0.9 ml. Water at an approximate temperature of 12°C flowed through the cell holder during all measurements, which prevented the sample from overheating and killing live animals. The stirrer maintained a suspension of the animals in the cuvette, where only a small proportion of the volume was in the path of the excitation light, such that a random assortment of animals was measured for each sequential step of the 3D analysis. The number of animals in the sample influenced the stability of the measurement, while too many animals would disrupt the suspension, too few animals would not provide a homogenous mixture. The number of animals needed for a stable measurement depended on the species, stage and ultimately the body size of the animals.

*Lepeophtheirus salmonis* samples contained a mean of 150 animals, while non-target copepod samples contained between 25 (late stage *Centropages* spp.) and 250 (*Oithona* spp.) animals. Metadata for each formalin and live sample measured can be found in the supplementary material (Table S1). All *L. salmonis* and *C. elongatus* samples comprised animals from a single stage and age. Non-target copepod spp. were sorted to genus, and samples contained a mix of copepodid and adult stages. Less than an hour prior to measurement, animals stored in formalin were removed from preservation with a sieve, transferred through two filtered salt water rinses using a pipette and then transferred to the cuvette.

Fluorescence intensity was influenced by the fluctuating number of animals in the path of the excitation beam during the 5-min measurement. We compensated for this artefact by repeating measurements of each sample five times, calculating the mean and applying a smoothing function, which found the median value within 10 nm. The fluorescence intensity was further normalized on a 0- to 1-point scale by dividing intensity by the maximum fluorescence within each EEM measurement. EEM measurements made on animals stored in ethanol were highly variable between samples of the same species. Further examination suggested that the fluorophore, which originates from *L. salmonis,* leaches into the ethanol solution, separating the fluorescence signal from the animal (Figure S1). Thus, ethanol preservation hinders the identification and enumeration of the animals and ethanol EEM measurements were therefore excluded from further analysis. EEM data were processed in MATLAB using the *drEEM* toolbox to assemble the data set, apply scale transformations, remove Rayleigh and Raman scatter, and produce figures (Murphy et al., 2013).

## 2.3 | Spectrum section analysis of EEM measurements

Fluorescence peaks (uniquely high fluorescence intensity at a specific conjunction of an excitation (Ex.) and emission (Em.) wavelength) were identified from the EEM data set through a systematic sectioning of the excitation wavelengths into 20-nm wide bands centred on the focus wavelength. Fluorescence intensity within each section was normalized to the maximum intensity and evaluated for the relative fluorescence intensity difference between a target group of lice samples and non-target copepod samples, which served as comparators. The lice samples were divided into 4 target groups: "Nauplii" (N1 and N2 stages combined), "Young Copepodid" (sampled 6 DPH) and "Old Copepodid" (sampled 12 DPH), which both originated from *L. salmonis* maintained on Atlantic salmon (*Salmo salar),* and "Sea Trout Copepodid" (sampled 6 DPH), which were *L. salmonis* that originated from wild-caught *Salmo trutta.* Since the duration of formalin storage affects fluorescence intensity in target *L. salmonis* copepods [see section 3.2.2, Formalin storage and fluorescence intensity], the EEM data set was limited to those target copepod samples that had been in storage for more than 60 days. The non-target copepod samples included in the analysis were in formalin storage for 7 days or more prior to measurement, and the *C. elongatus* samples were 33 days in formalin storage when measured.

The young copepodid samples were chosen as the target group for identifying excitation section peaks (the maximum fluorescence intensity found within each excitation section, specified as a conjunction of Ex. and Em. wavelengths). At each excitation section peak ($\pm$10 nm), the mean difference in relative intensity between target group and non-target copepod comparators was calculated as the *peak intensity distance*. The peak intensity distances of each excitation section were then evaluated to manually select the fluorescence peaks where the greatest and most reliable fluorescence difference between the lice target groups and non-target copepod comparators occurred. The fluorescence peaks that appeared to best differentiate target from non-target copepods were identified and selected for further analysis.

## 2.4 | Fluorescence microscopy

Fluorescent images of individual animals were taken with a Nikon DS-Fi3 on an inverted Nikon Eclipse Ti Microscope using three CHROMA filter sets: DAPI, Ex. 350 $\pm$ 50 nm and Em. 460 $\pm$ 50 nm; EGFP (FITC/Cy2), Ex. 470 $\pm$ 40 nm and Em. 525 $\pm$ 50 nm; and CY3/TRITC, Ex. 545 $\pm$ 25 nm and Em. 605 $\pm$ 70 nm (illustrated in Figure 2). The Nikon software NIS-Elements controlled operations and settings for the camera and microscope. Fluorescence saturation was avoided by setting the power of the Lumencor SOLA Light Engine to 25% for images taken with the DAPI and CY3/TRITC filter sets, while it was set to 5% for the EGFP filter set, and all other settings were kept the same. Observations were made using a glass-bottomed dish with a 0.16- to 0.19-mm-thick borosilicate glass base. Animals from

formalin samples were handled in the same manner as during the EEM measurements, that is removed from preservative, rinsed and placed in filtered sea water. Live animals were placed in a solution of filtered sea water and methyl cellulose, which inhibited their movement but did not produce any fluorescence in the spectra measured.

Image processing and analysis were conducted with Java and R, respectively. Fluorescence was recorded as an RGB image value with a 0 (black) to 255 (white) greyscale serving as a proxy for intensity (Figure 1). In each channel, the pixels with a value below a threshold set to 5 were disregarded and the number of pixels above the threshold was counted, and their greyscale values were summed. Across the three channels, the number of pixels and their total value were recorded, which gave a measure of total fluorescence intensity and the area fluorescing for each animal. The fluorescence was then analysed according to storage duration, animal size, sea louse species, origin and host fish, development stage, storage temperature and animal age. Linear regression and statistical tests including ANOVA and paired *t* tests specified in the results section were carried out using packages in the R software environment (R Core Team, 2018).

## 3 | RESULTS

### 3.1 | Spectrum section analysis of EEM measurements

EEM measurements showed that the fluorescence profile of *L. salmonis* differed broadly from non-target copepod spp. examined (Figure 2). Although all samples exhibited a wide fluorescence peak near Ex. 290 nm and Em. 320 nm, *L. salmonis* EEM measurements also featured increased fluorescence at higher wavelengths that was absent in other included species. Most non-target copepod measurements, including those of *Acartia* spp. (Figure 2c,f), lacked fluorescence in those higher wavelengths, while some species, such as *Temora* spp. (Figure 2b,e), exhibited fluorescence in this area, but at lower intensities. The fluorescence profiles of the live samples were less dynamic and of lower intensity than those stored in formalin, and the fluorescence profile of *L. salmonis* further varied in relation to stage, age of the animal, host fish and duration of formalin preservation. Those patterns of fluorescence were examined through spectrum section analysis of EEM measurements and fluorescence microscopy [section 3.2]. The spectrum section analysis data set included EEM measurements of live samples (Figures 3a and 4), target *L. salmonis* samples that had been in formalin storage for 60 days or longer, and non-target copepod samples that had been in formalin storage for more than 7 days (Figures 3b and 5). Spectrum section analysis found that peak intensity distance was greatest in excitation sections higher than 300 nm in both live and formalin samples. In excitation sections below 290 nm peak intensity, distance between target groups and the non-target copepod comparators was inconsistent and occasionally turned negative with the lice target group having the lower intensity.

### 3.1.1 | Spectrum section analysis of live samples

Through the spectrum section analysis, Ex. 330 nm and Em. 418 nm were identified as the fluorescence peak best suited for distinguishing live *L. salmonis* from non-target copepod comparators (Figure 3a). The peak intensity distance of the young copepodid target group remained high between Ex. 310 and 420 nm, but fluorescence
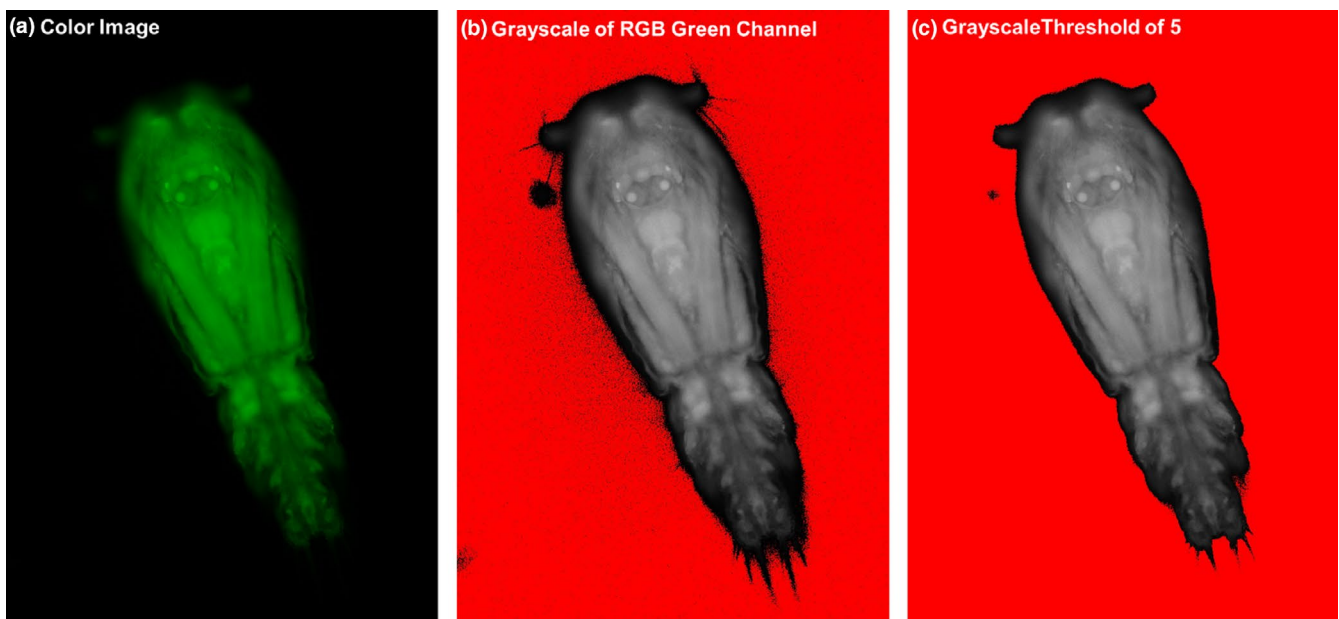


**FIGURE 1** Fluorescent image processing of *Lepeophtheirus salmonis* copepodid. (a) Colour image (cropped) taken with the GFP filter set. (b) The green channel of the colour image in greyscale with red colour having an RGB value of 0, black and dark grey have low RGB values, and whites have a high value. (c) Thresholding removes all pixels below a value of 5
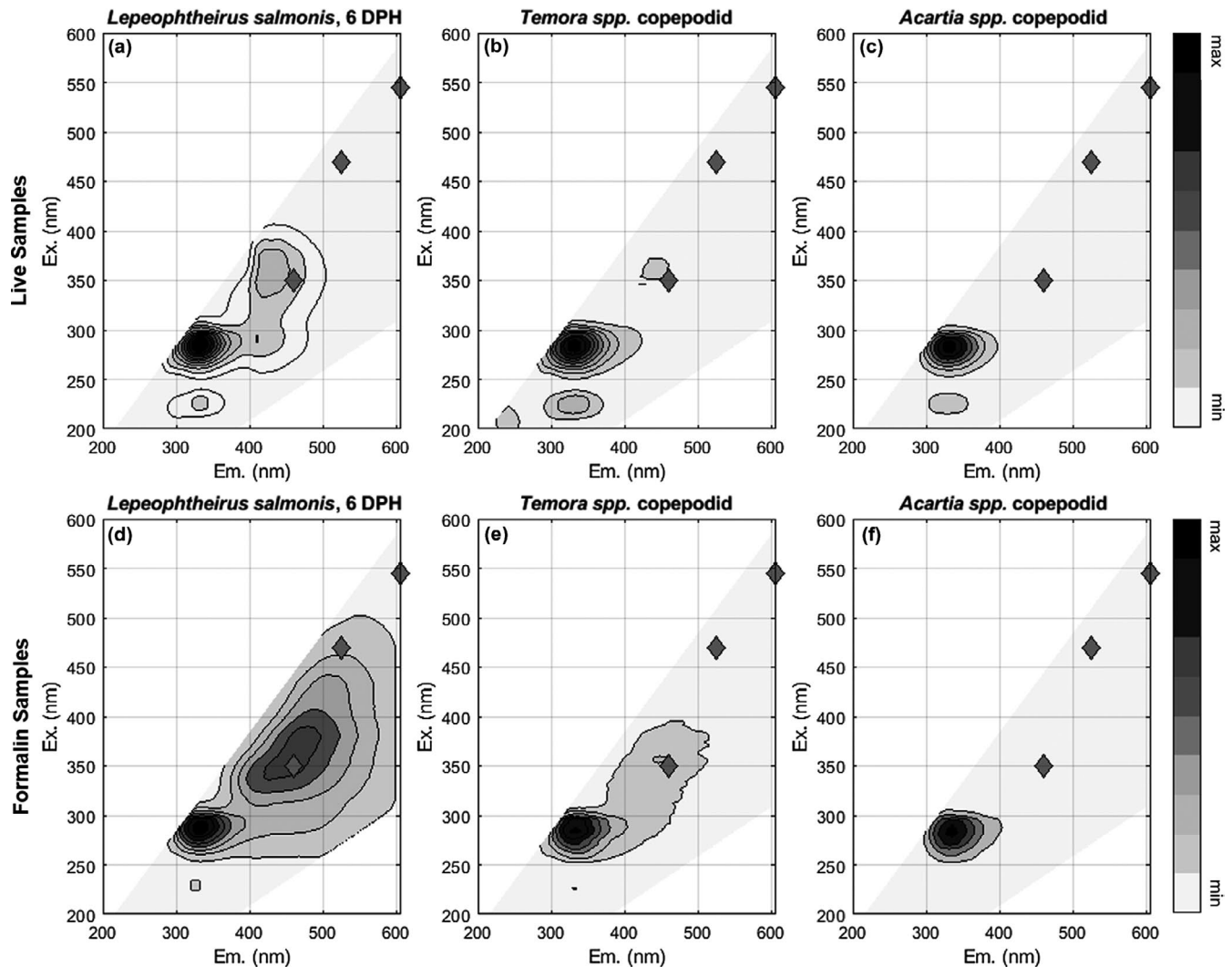
**FIGURE 2** EEM measurements of live and formalin-preserved copepods. The displayed EEM measurements are means of measurements taken for the listed species (a:f). *L. salmonis* copepodid samples were in formalin storage for 60 days prior to measurement. Emission and excitation wavelengths (nm) are indicated on the *x*- and *y*-axes, respectively. Normalized fluorescence intensity is depicted through the greyscale contouring with the darkest shade representing maximum fluorescence in the EEM for each species. The diamonds mark the centre wavelength of the filter sets: Ex. 350 ± 50 nm and Em. 460 ± 50 nm; Ex. 470 ± 40 nm and Em. 525 ± 50 nm; and Ex. 545 ± 25 nm and Em. 605 ± 70 nm [see section 3.2, Fluorescence Microscopy]

intensity decreased rapidly after Ex. 380 nm and the peak distance of the nauplii group became negative after 350 nm.

At the identified excitation section and fluorescence peak (Ex. 330 nm and Em. 418), the greatest fluorescence intensity was found in the young copepodids with a mean of 0.21, and the lowest was found in the non-target copepods and N1 *L. salmonis* with means of 0.037 and 0.043, respectively (Figure 4, Table S2). The mean intensity at the peak for sea trout copepodids was 0.17, 0.12 for old copepodids and 0.11 for N2 *L. salmonis* samples. The sea trout copepodid intensities were less than young *L. salmonis* copepodids but >4 times greater than the mean of non-target copepod samples, which was 0.04. The *C. elongatus* samples also exhibited greater fluorescence than the non-target samples with a mean intensity of 0.12 but had a lower intensity than the young *L. salmonis* copepodids.

### 3.1.2 | Spectrum section analysis of formalin samples

Spectrum section analysis of formalin samples indicated that there were many sections between 310 and 510 nm where target groups of *L. salmonis* could be distinguished from non-target copepods (Figure 3b). Along those wavelengths, the fluorescence intensity of the young copepodid group increased to a peak at 380 nm and then decreased through higher wavelengths. The peak intensity distance was lowest in the sea trout copepodid group, while it was the highest in the nauplii and young copepodid target groups. The peak intensity distance calculated for the old copepodid target group was lower than that of the highest groups, but followed the same pattern.

Closer inspection of two local peaks, Ex. 380 nm and Em. 474 nm and Ex. 450 nm and Em. 516 nm, exhibited the pattern in

**(a) Live Samples**
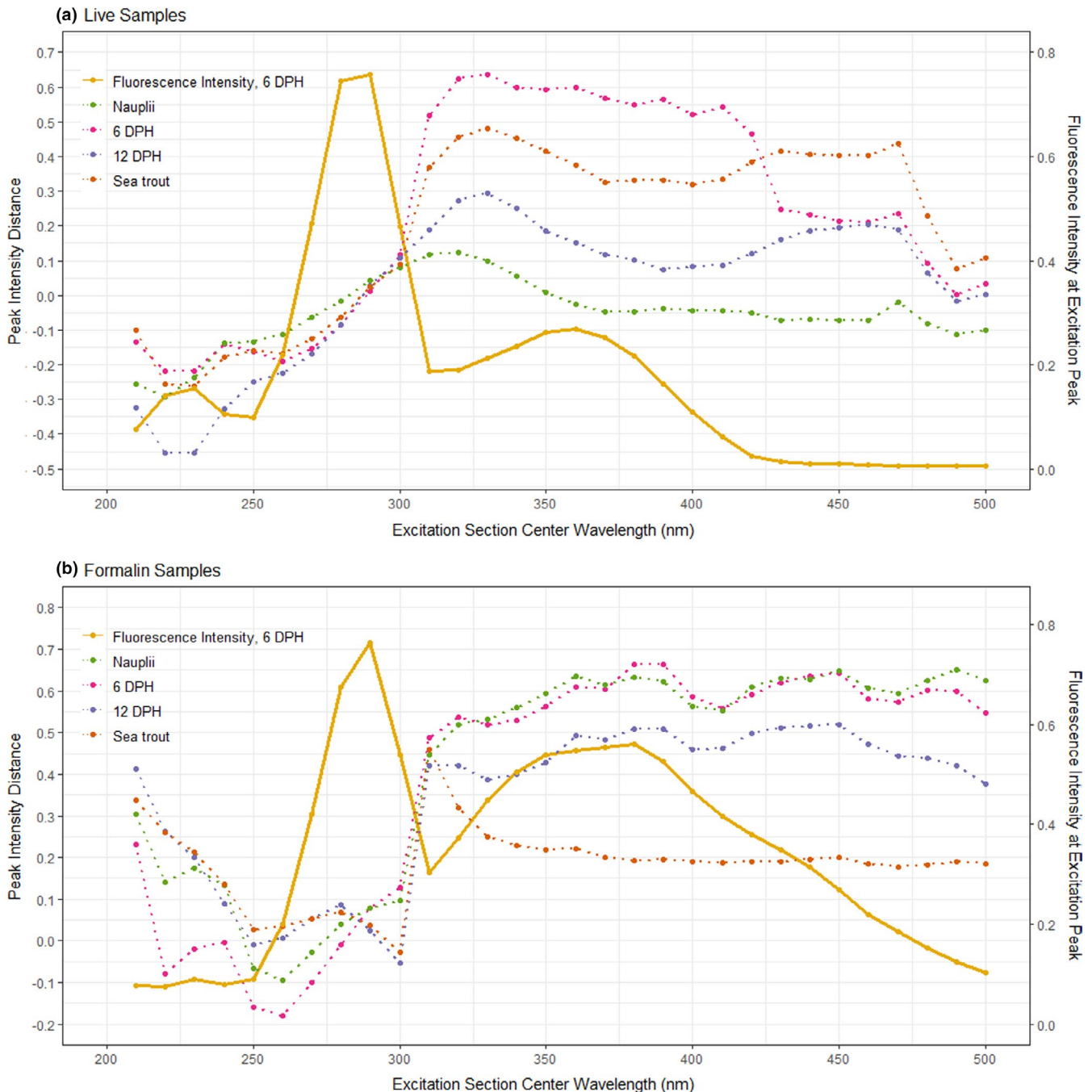


**(b) Formalin Samples**



**FIGURE 3** Fluorescence peaks identified through section analysis for (a) live samples and (b) formalin samples. The centre wavelength of the excitation section (±10 nm) is shown on the x-axis and the peak intensity distance on the y-axis. Peak distance is a calculation of the fluorescence intensity difference between the target group and non-target copepod comparators for the indicated excitation section peak. A second y-axis is included on the right side of graphs A and B, and the variable is depicted by the solid yellow line showing maximum fluorescence intensity of the young copepodid target group for the excitation section. Target groups "Nauplii, N1 and N2," "Young Copepodid" (sampled 6 DPH) and "Old Copepodid" (sampled 12 DPH) are *Lepeophtheirus salmonis* samples taken from *Salmo salar* host fish ,while "Sea Trout Copepodids" are 6 DPH *L. salmonis* samples from *Salmo trutta* host fish. All samples included in the Figure 3a and b graphs are also included in Figures 4 and 5, respectively

greater detail (Figure 5a,b, Table S2). Along both sections, the fluorescence intensities of nauplii (N1 and N2), young copepodid and old copepodid samples were greater than those of the non-target copepod samples. The highest mean intensities were found in the young copepodids at their respective fluorescence peaks, 0.61 (Ex. 380 ± 10 nm and Em. 474 ± 10 nm) and 0.29 (Ex. 450 ± 10 nm and Em. 516 ± 10 nm), while the means for non-target copepod samples were 0.09 (Ex. 380 ± 10 nm and Em. 474 ± 10 nm) and 0.02 (Ex. 450 ± 10 nm and Em. 516 ± 10 nm). The old copepodids had lower mean fluorescence intensities than the other *L. salmonis* from
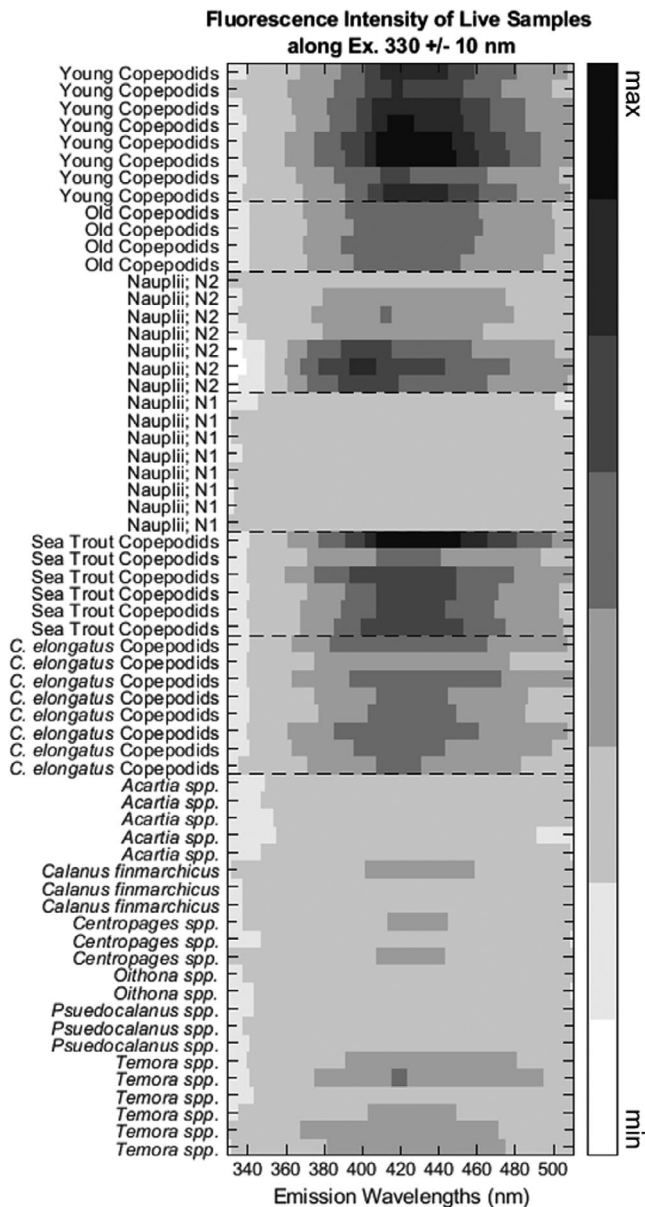
**FIGURE 4** Relative fluorescence intensity of live samples along 330 ± 10 nm excitation spectrum with the darkest shades indicating maximum intensity. Target groups "Young Copepodids" (sampled 6 DPH), "Old Copepodids" (sampled 12 DPH) and "Nauplii, N1 and N2" are *Lepeophtheirus salmonis* samples taken from *Salmo salar* host fish, while "Sea Trout Copepodids" are 6 DPH *L. salmonis* samples from *Salmo trutta* host fish. "*C. elongatus* Copepodids" (sampled 6 DPH) were taken from *Salmo salar* host fish. Apart from *Calanus finmarchicus*, non-target copepod samples were identified to genus

*Salmo salar* hosts, with 0.49 (Ex. 380 ± 10 nm and Em. 474 ± 10 nm) and 0.24 (Ex. 450 ± 10 nm and Em. 516 ± 10 nm), but those means were distinctly higher than the non-target copepod samples. The sea trout copepodid samples were occasionally indistinguishable from the non-target copepod samples with some having lower intensity than the *Temora* spp. measurements. Likewise, *C. elongatus* fluorescence was not distinguishable from the non-target copepod fluorescence.

## 3.2 | Fluorescence microscopy

While each animal was imaged with all three filter sets, the following analysis focused on the formalin samples with the EGFP measurements (Ex. 470 ± 40 nm and Em. 525 ± 50 nm). The EGFP filter set includes the best performing fluorescence peak identified by the spectrum sectioning analysis: Ex. 450 ± 10 nm and Em. 516 ± 10 nm (Figure 3). Images of *L. salmonis* showed that fluorescence was widespread in the louse tissue with increased concentration in the eyespots and the maxillae (Figure 2). Non-target copepods similarly displayed widespread, but weaker, fluorescence with occasional areas in the gut or lipid sacs where fluorescence intensity was elevated.

### 3.2.1 | Total fluorescence and animal size

Total fluorescence intensity increased with animal size as measured by the number of fluorescent pixels above the threshold (Figure 6). The *L. salmonis* were raised under controlled laboratory conditions and were all at the same developmental stage and age, resulting in little variation in size. Meanwhile, the animals in the non-target copepod measurements were more variable in size due to the inclusion of several species in various developmental stages. Fitting the non-target copepod data to a linear regression, with total pixels as the independent variable and total fluorescence intensity as the dependent variable, resulted in the formula $f(x) = -6.29^*10^6 + 38.1x$ ($R^2 = 0.77$). A linear regression fit to measurements of laboratory-cultured *L. salmonis* copepodids that had been in storage for over 30 days resulted in the formula $f(x) = -1.02^*10^{68} + 186x$ ($R^2 = 0.47$). The number of fluorescing pixels did not change in relation to storage duration according to an ANOVA performed on the data set of *L. salmonis* measurements in storage for greater than 30 days ($F_{1,116} = 0.724$, $p = .396$). Thus, mean fluorescence intensity can be calculated from total fluorescence intensity and total number of fluorescing pixels for each animal imaged in order that further analysis be conducted.

### 3.2.2 | Formalin storage and fluorescence intensity

The mean fluorescence intensity of laboratory-grown salmon lice increased with storage duration in formalin (Figure 7). A saturation curve with the formula $f(t) = 84.09t/6.57+t$ was found to have the best fit with an $R$-squared of 0.867 (RMSE = 8.40). According to the formula, the mean intensity is 69.1 at day 30 and 75.8 at day 60, 82.0% and 90.1% of the asymptote maximum, respectively. Since the intensity rapidly increases in the first 30 days of storage and more slowly thereafter, significance tests were only performed on lice data sets from equivalent timeframes greater than 30 days. *C. elongatus* were measured at two formalin storage duration time points, day 33 and day 133, and their mean fluorescence intensities were 50.2 and 54.7, respectively. While the
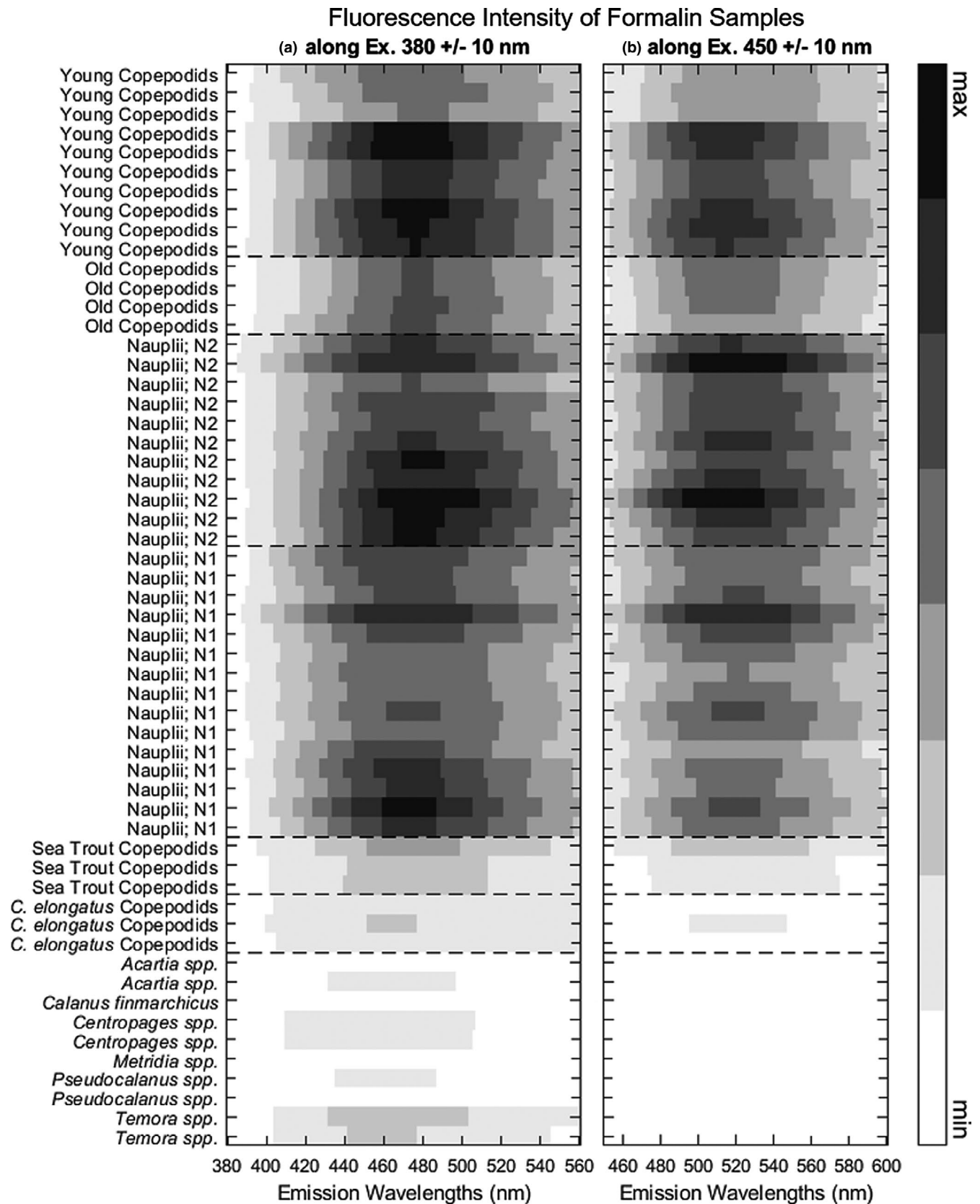
**FIGURE 5** Relative fluorescence intensity of formalin samples along (a) 380 ± 10 nm and (b) 450 ± 10 nm excitation spectra with the darkest shades indicating maximum intensity. Target groups "Young Copepodids" (sampled 6 DPH), "Old Copepodids" (sampled 12 DPH) and "Nauplii, N1 and N2" are *Lepeophtheirus salmonis* samples taken from *Salmo salar* host fish, while "Sea Trout Copepodids" are 6 DPH *L. salmonis* samples from *Salmo trutta* host fish. "*C. elongatus* Copepodids" (sampled 6 DPH) were taken from *Salmo salar* host fish. All target group samples were in formalin storage for greater than 60 days, except *C. elongatus*, which was in storage 33 days. Apart from *Calanus finmarchicus*, non-target copepod samples were identified to genus. Non-target samples were in formalin storage for more than 7 days
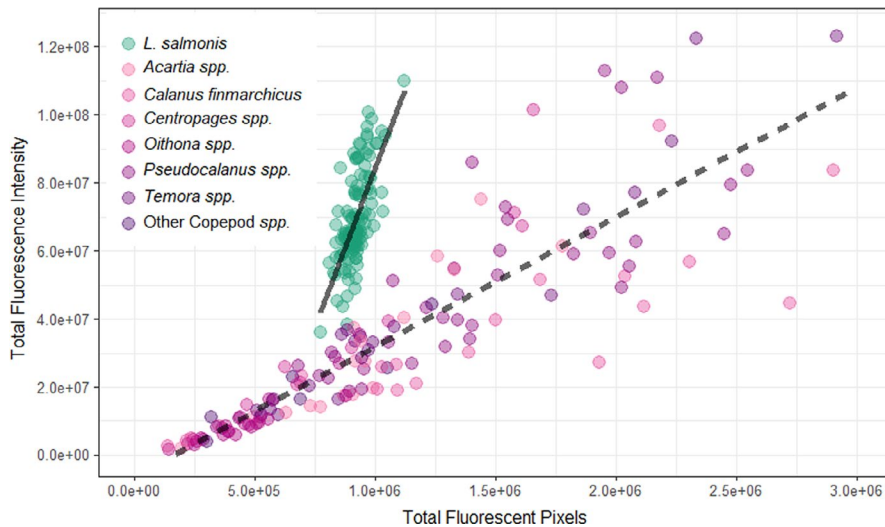
**FIGURE 6** Relationship between fluorescence intensity and number of fluorescing pixels, measured with the EGFP filter set (FITC/Cy2), Ex. 470 ± 40 nm and Em. 525 ± 50 nm. Lines for linear regressions of *Lepeophtheirus salmonis* data (solid) and non-target copepod species data (dashed). Points depict single measurements, and colours indicate species. All *L. salmonis* data are from 6 DPH copepodids from laboratory-cultured salmon (IMR, Norway)
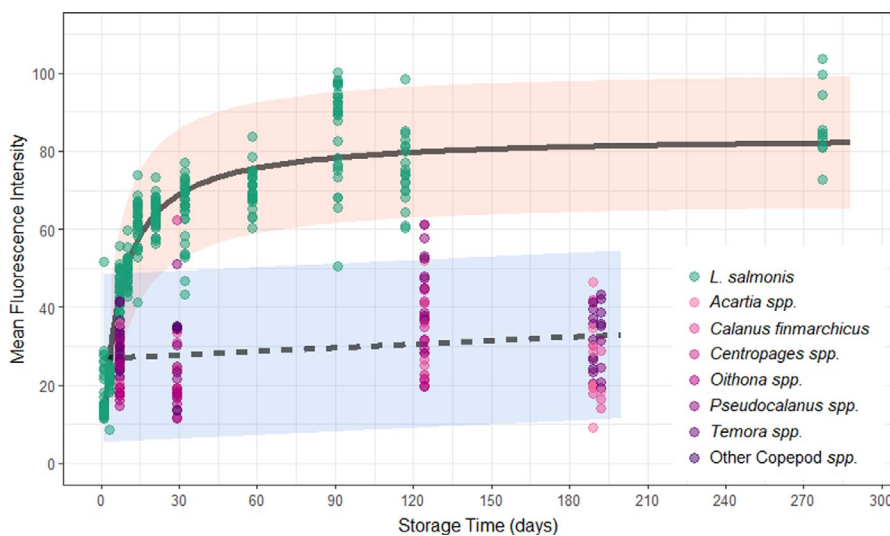


**FIGURE 7** Relationship between mean fluorescence intensity (total intensity / pixels counted) and storage time in formalin, measured with the EGFP filter set (FITC/Cy2), Ex. 470 ± 40 nm and Em. 525 ± 50 nm. All *Lepeophtheirus salmonis* data are for 6 DPH copepodids from laboratory-cultured salmon (IMR, Norway). Points depict single measurements, and colours indicate species. 95% prediction intervals are indicated with shaded regions for the saturation curve fit to *L. salmonis* data and linear regression fit to non-target copepod spp. data

mean fluorescence intensity of *C. elongatus* measured on the latter date was greater, there were not enough storage duration data points to perform any further analysis in relation to formalin storage duration.

The fluorescence intensity of non-target copepods exhibited a significant, but weak linear relationship with storage duration in formalin ($R^2$ = 0.039, $p$ = .0134) (Figure 7). Since storage duration of non-target copepods did not explain much of the variability in fluorescence intensity, we performed an ANOVA including the entire non-target copepod spp. data set (mean ± $SE$ = 29.5 ± 0.93, $n$ = 139) and the measurements of laboratory-grown salmon lice that had been in storage for over 30 days (mean ± $SE$ = 75.3 ± 1.14, $n$ = 118). The fluorescence intensity of non-target copepods was significantly different from the salmon lice ($F_{1,256}$ = 982, $p$ < .001). However, the variance in mean fluorescence intensity may result in the occasional measurement of a *L. salmonis* copepodid below that of a non-target copepod. At 30 days in formalin, the lower bound of the 95% prediction interval for salmon lice copepodids was 52.2, while the upper bound for the non-target copepods was

49.3. Although the 95% prediction intervals do not overlap, 4.3% (6/139) of the non-target copepods had a mean fluorescence intensity over 52.2, and 1.7% (2/118) of the *L. salmonis* copepodid measurements were below 49.3.

### 3.2.3 | Factors influencing the fluorescence profile

Several factors were investigated to determine their relationship to the measured fluorescence intensity of the animal, including sea louse species, origin and host fish; development stage; storage temperature; and age (Figure 8). In all cases, the pattern of intensity, as influenced by the factor, is specific to the spectrum of fluorescence examined. The following analysis focused on the data set derived from the EGFP filter set. Within each factor, $t$ tests were performed between a reference group and the various other categories presented, except for the age comparison in which the $t$ test was performed for each filter set. Descriptive statistics and the Bonferroni-adjusted $p$-values for each significance test are provided in full in Table S3.
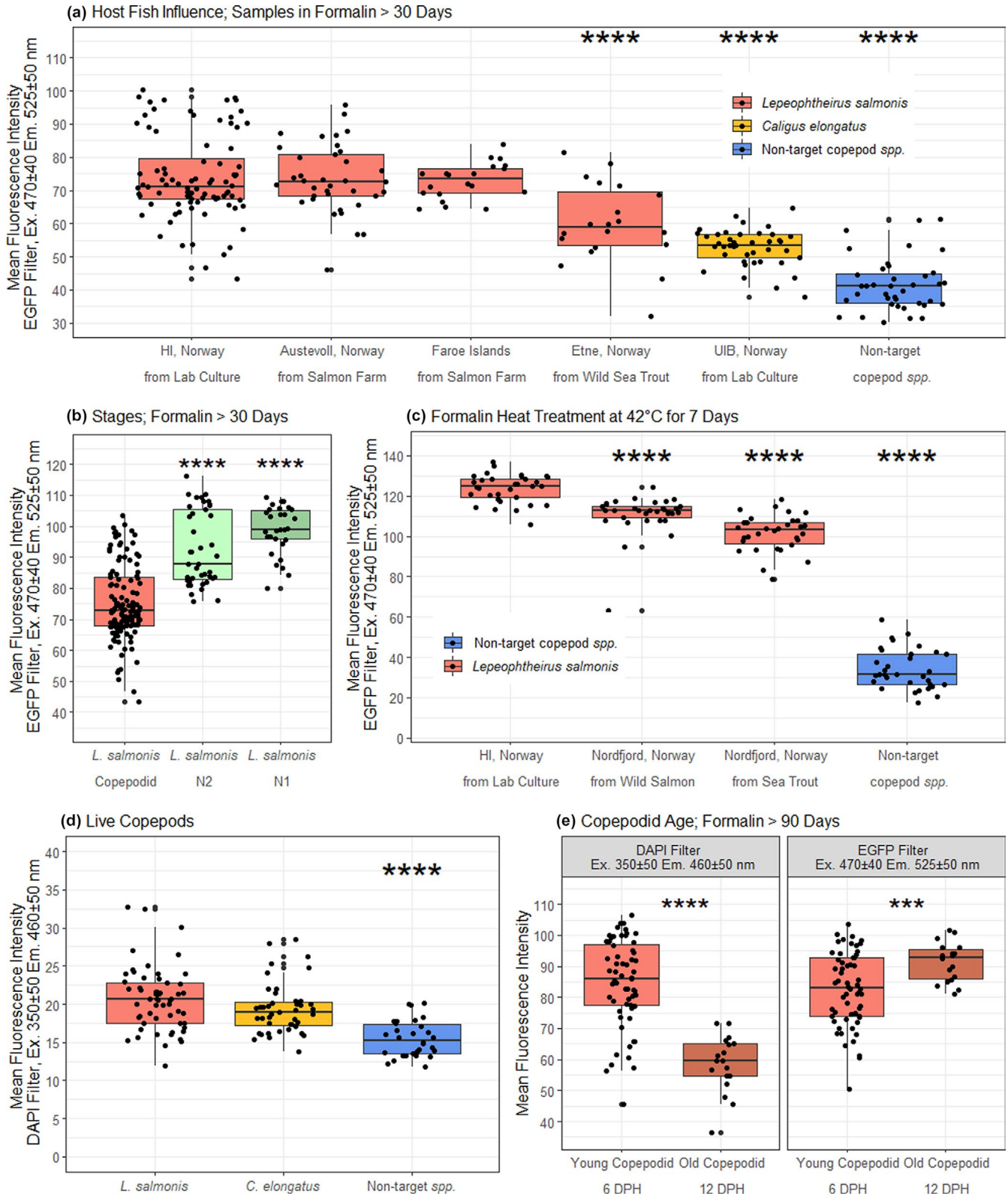
**FIGURE 8** Factors influencing the mean fluorescence intensity (total fluorescence intensity / total number of fluorescing pixels) analysed by factor category (a–e) with selected reference category for *t* tests placed on the left side of each box plot, except for (e) in which the *t* test was performed for each filter set. Asterisks indicate Bonferroni-adjusted *p*-values (****<.00001 and ***<.0001)

*Host fish* (Figure 8a): Measurements of *L. salmonis* copepodids, which had been in formalin storage more than 30 days, were analysed according to their host fish origin. No significant differences were found between copepodids originating from Atlantic salmon hosts raised under laboratory conditions or taken from a farm. *C. elongatus* taken from laboratory-raised salmon and *L. salmonis* found on wild-caught sea trout were significantly different from the laboratory-cultured *L. salmonis* ($p$-value $<$ .00001). Although they exhibited lower mean fluorescence intensity, they were both significantly greater than the non-target copepods ($t$ test, $p <$ .00001). Specifically, laboratory-reared *L. salmonis* mean fluorescence intensity is 1.4 times greater than *C. elongatus*, while *C. elongatus* mean fluorescence is 1.6 times greater than the non-target copepods.

*Stages* (Figure 8b): Measurements of samples, which had been in formalin storage more than 90 days, showed developmental stage of *L. salmonis* significantly affected the mean fluorescence intensity ($p <$ .00001). Nauplius stages N1 and N2 exhibited greater fluorescence per pixel than the copepodid stage, with 98.7, 91.3 and 75.3, respectively. However, no significant difference was found between the stages when examining the total fluorescence intensity (ANOVA: $F_{2,189} = 1.86$, $p =$ .158).

*Heat treatment* (Figure 8c): Laboratory-cultured 6 DPH *L. salmonis* copepodids stored at 22°C for 7 days had a mean fluorescence intensity of 44.6, while those stored at 42°C for 7 days had 124, a 2.8 factor increase (Table S3). The heat-treated copepodids from the laboratory culture had significantly greater mean fluorescence intensity than heat-treated copepodids from both wild-caught *Salmo salar* and *Salmo trutta* hosts ($p <$ .00001). Their mean fluorescence was also found to be significantly greater than heat-treated non-target copepods by a factor of 3.6 ($p <$ .00001). Meanwhile, the mean fluorescence intensity of *L. salmonis* copepodids from wild-caught *Salmo salar* and *Salmo trutta* was 3.3 and 3.0 times greater than the heat-treated non-target copepods ($p <$ .00001).

*Live copepods* (Figure 8d): The fluorescence peak at Ex. 330 nm and Em. 418 nm was identified by the spectrum sectioning analysis as the best peak for distinguishing live *L. salmonis* from non-target copepod spp. The peak is located within the spectrum covered by the DAPI filter set (Ex. 350 ± 50 nm and Em. 460 ± 50 nm). Measurements taken with the DAPI filter set showed that mean fluorescence intensity of 6 DPH *L. salmonis* copepodids was significantly different from the non-target copepods. ($p <$ .00001), but they were not significantly different from *C. elongatus* copepodids ($p =$ .0977). The mean fluorescence intensity of the live *L. salmonis* copepodids was 1.06 times greater than live measurements of non-target copepods. Meanwhile in 30-day-old formalin samples measured with the EGFP filter, the mean fluorescence intensity of *L. salmonis* measurements was 2.25 times greater than the mean of non-target copepod samples (Figure 7). Thus, the relative difference between salmon lice and non-target copepod spp. in live samples is much less than that found in formalin samples.

*Copepodid age* (Figure 8e): Amongst samples that had been in formalin storage for more than 90 days, the DPH of *L. salmonis* copepodids significantly affected the fluorescence intensity in both the DAPI and EGFP filter data sets ($p <$ .0001), but in opposite directions. In the DAPI data set, the mean fluorescence intensity of 6 DPH copepodids was 1.45 times greater than the 12 DPH mean fluorescence intensity. In the EGFP data set, 6 DPH copepodids differed from 12 DPH copepodids by a factor of 0.9.

## 4 | DISCUSSION

Collection of EEM data facilitated the identification of fluorescence peaks where intensity differences could be used to differentiate between target sea lice species and non-target copepod spp. Once those peaks were identified, further work employing fluorescence microscopy assessed the strength of the fluorescence signal and its reliability in response to influencing factors. The EEM measurements could not be utilized for that analysis or to calculate the absolute differences in fluorescence between samples because the intensity was normalized to the maximum, since the exact number of individuals measured could not be practically controlled. However, the EEM measurements efficiently resolved the fluorescence profiles of the various species and treatments examined, whereas fluorescence microscopy is limited to wavelength combinations defined by the filters used. Together, the exploration of fluorescence profiles with EEM measurements and the assessment of signal strength with fluorescence microscopy demonstrated that *L. salmonis* can be distinguished from non-target copepod spp. using fluorescence.

### 4.1 | Spectrum section analysis of EEM measurements

The spectrum section analysis provided a means of systematically processing the EEM measurements in a manner that mimicked the use of microscopy excitation filters and emission filters. Evaluating the intensity difference between EEM samples at each conjunction of excitation and emission wavelengths is also more economical than doing the same with many different filters. Rather than examining all possible combinations, the analysis focused on the points at which *L. salmonis* copepodids exhibited the greatest fluorescence and where their fluorescence would be greater than other animals. The target *L. salmonis* nauplii and copepodids could also be distinguished from other zooplankton where they had a lower fluorescence intensity, as seen with the negative peak intensity distances in wavelengths below 290 nm. Nielsen et al. (2019) similarly demonstrated that when using a 410-nm excitation light several zooplankton species exhibit a fluorescence peak at an emission wavelength of 686 nm, but not *L. salmonis*. The negative signal was due to fluorescence of chlorophyll consumed by the grazing zooplankters in contrast to the non-feeding *L. salmonis*. A negative signal might be useful in an automated process as argued by Nielsen et al. (2019), but it would not be useful in enumerating animals via a fluorescence modification of traditional light microscopy methods in which the animal must standout against the darkfield (as described by Bui

et al., 2020). Thus, wavelengths above 600 nm, where chlorophyll fluoresces, were not examined here and the spectrum section analysis identified the wavelengths with greatest positive peak intensity distance.

The EEM measurements characterized the fluorescence profiles of each copepod species and indicated the difference in fluorescence intensities between them. However, the relative difference observed in the EEM measurements between two species was occasionally contradicted by the fluorescence microscopy data. The mean fluorescence intensity of the live 6 DPH *L. salmonis* copepodids (*Salmo salar* host) was 4.8 times greater than the non-target copepods in the EEM measurements, but only 1.06 times greater in the fluorescence microscopy data using the EGFP filter set (Ex. $470 \pm 40$ nm and Em. $525 \pm 50$ nm). Likewise, in the formalin-fixed samples the mean fluorescence intensity of 12 DPH *L. salmonis* copepodids was higher than that of the 6 DPH group when measured by fluorescence microscopy (Ex. $470 \pm 40$ nm and Em. $525 \pm 50$ nm), but the relationship was reversed when looking at the same groups using the EEM measurements. Since the EEMs are normalized to the maximum fluorescence peak, usually near Ex. 290 nm and Em. 320 nm, an increased or decreased intensity, there would decrease or increase the normalized amount elsewhere. Thus, the EEMs were not direct measures of quantitative differences in fluorescence, so further fluorescence microscopy was required to validate these differences.

## 4.2 | Fluorescence microscopy

Mean fluorescence intensity was calculated for each animal so that comparisons could be made across species and treatments, but the total number of fluorescing pixels is also a useful signal. In automated processing of images, particle size (total pixels) could help distinguish *L. salmonis* from other species, which have comparable mean fluorescence intensities. Otherwise, false-positive identifications could occur if only using the mean intensity. Despite the large overall difference in mean intensities between formalin-preserved *L. salmonis* and non-target copepod species, overlap did occur between the animals imaged with the EGFP filter set (Ex. $470 \pm 40$ nm and Em. $525 \pm 50$ nm). Considering the relative rarity of *L. salmonis* in the water column, false positives could quickly become problematic, and using both mean fluorescence and total size may not be sufficient to prevent such occurrences. A second fluorescence signal, such as the negative chlorophyll signal suggested by Nielsen et al. (2019), might provide enough additional information to facilitate a fully automated detection system. Alternatively, nominal detection could be confirmed through morphological inspection of the animal. As *L. salmonis* are relatively unique in their appearance, positive identification could be quickly accomplished. Similarly, simple shape analysis / classification would likely prove sufficient to discriminate between problem specimens. Although only one fluorescence filter set can be used as an aid to traditional taxonomic methods at any time, the unique morphology of *L. salmonis* could thus be used for positive identification after locating the illuminated animal.

## 4.2.1 | Formalin fixation: storage time and temperature

The strong fluorescence signal in the formalin samples indicates that chemical reactions occur during fixation between the tissues and the formaldehyde to create fluorophores. The fluorophores generated are unknown, but the fluorescence signal shows that some of them are unique to *L. salmonis*. Formaldehyde fixation is a complex process that occurs in three steps: the initial penetration of the tissue, followed by covalent bonding of the formaldehyde with the tissue, and then cross-linking (Buesa, 2008). Penetration is rapid, while the binding may take 24 hr or more depending on the thickness of the tissue and the storage temperature (Fox et al., 1985). The formaldehyde binding can occur with any group containing a reactive hydrogen atom, but the rate varies considerably with amine reactivity being fastest. Cross-linking then occurs progressively with potential functional groups forming methylene bridges in a process that can continue for months or years (Dapson, 2010). Thus, the increase in fluorescence intensity of *L. salmonis* samples with storage time can be explained by the slow process of cross-linking. The heat treatment increases the rate of this reaction and the total number of fluorophores as shown by the greater fluorescence intensity. Although evaluating the mechanism is beyond this study, heating apparently changes the reaction equilibrium towards creation of a greater number of fluorophores. Rather than increasing the number of fluorophores, an alternative explanation could conclude that over time or through the heat treatment, new highly fluorescent fluorophores are created. Future studies that seek to enumerate *L. salmonis* through fluorescence should only process formalin samples, which have been stored at room temperature for greater than 3 months or should apply a heat treatment prior to examination.

## 4.2.2 | Factors influencing the fluorescence profile

While storage temperature affects the reactions occurring during fixation, the other factors examined relate to the endogenous macromolecules, which constitute the compounds forming fluorophores. Since the planktonic stages are non-feeding, they are dependent upon their maternally derived storage lipids for energy, which decrease in volume over time, as does carbon mass (Brooker et al., 2018; Gravil, 1996; Thompson et al., 2019). The fatty acid composition of storage lipids varies with maternal origin (Tocher et al., 2010), the incubation temperature and age (Skern-Mauritzen et al., 2020), and development stage (Thompson et al., 2019). Furthermore, at least three proteins in nauplii have been demonstrated to be of maternal origin (Dalvin et al., 2009, 2011). Thus, the composition of proteins and lipids in the animal is dependent on several factors. Some of those factors have been categorized and examined here, and their influence was reflected in the fluorescence patterns observed.

Old *L. salmonis* copepodids fluoresced at lower intensities than younger copepodids when using the DAPI filter set (Ex. $350 \pm 50$ nm and Em. $460 \pm 50$ nm), which suggests that the responsible

fluorophore is related to energy stores or an otherwise decreasing entity. Meanwhile, the same comparison made with the EGFP filter set (Ex. 470 ± 40 nm and Em. 525 ± 50 nm) yields a small increase in fluorescence and suggests the opposite. Therefore, the responsible fluorophore in the latter case is a robust fluorescence signal for detecting *L. salmonis* in samples where age cannot be controlled. When examining stage differences, the stability of the fluorophore is further demonstrated by N2 and N1 having progressively greater mean fluorescence intensity than the copepodids. The decrease in mean fluorescence intensity from N1 to copepodid can be explained by an increase in size with no change in total intensity, which indicates that there is no substantive change in the amount of fluorophore present.

No difference in fluorescence intensity was found between *L. salmonis* originating from laboratory cultures or farmed fish, but those from wild fish fluoresced less. The heat treatment further emphasized the trend, with laboratory-cultured *L. salmonis* fluorescing the most, followed by wild *Salmo salar* hosts and then wild *Salmo trutta* hosts. Following the maternal origin of lipids and proteins previously discussed, host fish diet is a possible influencing factor on fluorescence, but the intensity trend does not follow the gross dietary sources for each host fish category. Adult wild *Salmo salar* returning from the sea have a diet of wholly marine origin, while marine sources comprise 34%–89% of *Salmo trutta* diets (Davidsen et al., 2017), and the feed of farm raised and cultured *Salmo salar* is just 25% marine (Aas et al., 2019). A specific dietary component may still be responsible, or population-level differences between the host fish may be the cause of the fluorescence intensity differences. The lack of difference between the laboratory culture and the farm sites in Norway and the Faroe Islands indicates that genetic and temperature differences amongst the *L. salmonis* are not likely to be responsible. However, genetic variation within the Atlantic populations of *L. salmonis* is low (Glover et al., 2011), and further examination would be needed prior to application to a different population such as the Pacific subspecies (Skern-Mauritzen et al., 2014). Furthermore, the fluorescence signal exhibited by *L. salmonis* is not commonly shared by sea lice, as evidenced by the much lower fluorescence intensity in *C. elongatus*.

## 5 | CONCLUSION

The fluorescence signal induced by formalin fixation appears to be a reliable differentiator of planktonic *L. salmonis* in mixed zooplankton samples. A statistical difference was also observed between *L. salmonis* and non-target copepod spp. in live samples, but the small increase in fluorescence is not likely to be sufficient for routine identification. A modification of traditional taxonomic methods with fluorescence would aid in the locating and identifying of *L. salmonis* in formalin samples, greatly reducing processing times. Automated identification is also possible through the use of fluorescence, but multiple filter sets would be needed along with copious training of machine learning algorithms. While the development of a rapid identification method using fluorescence is motivated by the specific

problem of *L. salmonis*, the work exemplified here could be replicated for other purposes.

The non-target copepod spp. examined here are commonly found in the zooplankton assemblage along with the relatively rare *L. salmonis*. However, not all common copepod species were examined, such as *Metridia* spp. and *Microcalanus* spp., nor were the many other less common copepod species, cryptic species and non-copepod zooplankton examined. Any number of species with an unknown fluorescence profile could be found in a mixed zooplankton sample along with *L. salmonis*. While the non-target copepod spp. herein provided useful comparators for examining the differences in fluorescence to *L. salmonis*, they did not constitute an exhaustive survey. Considering the number and variability of species present in any given zooplankton sample, it would be impractical to individually assess the fluorescence profiles of all species. Instead, we suggest that the reliability of a fluorescence identification method could be assessed with trials on a variety of zooplankton samples spiked with a known number of salmon lice.

## CONFLICT OF INTEREST

The authors declare no conflict of interest, financial or otherwise.

## ETHICAL APPROVAL

All applicable international, national and/or institutional guidelines for the care and use of animals were followed. *Lepeophtheirus salmonis* is a copepod and unregulated by the animal use in research regulations in Norway or the European Union. Animal welfare was supervised by the Norwegian Food Safety Authority (Mattilsynet), with the Bergen salmon louse culture covered by approval number 11912 and NALO salmonid monitoring work covered by approval number 14809.

## DATA AVAILABILITY STATEMENT

Summary data tables corresponding to data presented in figures are included in the supplementary material of this article. The excitation and emission matrix (EEM) measurements were taken with the proprietary software "LabSolutions RF" and processed in MATLAB to produce the figures and data presented. EEM metadata are included in Table S1, and the corresponding EEM measurements can be found in Zenodo at https://doi.org/10.5281/zenodo.4157041 (Thompson et al., 2020).

## ORCID

_Cameron R. S. Thompson_ https://orcid.org/0000-0003-3318-4064

_James E. Bron_ https://orcid.org/0000-0003-3544-0519

_Samantha Bui_ https://orcid.org/0000-0002-7885-2989

_Sussie Dalvin_ https://orcid.org/0000-0002-6092-4710

_Mark J. Fordyce_ https://orcid.org/0000-0002-7899-5445

_Tomasz Furmanek_ https://orcid.org/0000-0001-8577-9604

_Gunnvør á Norði_ https://orcid.org/0000-0003-1550-6007

_Rasmus Skern-Mauritzen_ https://orcid.org/0000-0002-6983-8907

## REFERENCES

á Norði, G., Simonsen, K., Danielsen, E., Eliasen, K., Mols-Mortensen, A., Christiansen, D. H., Steingrund, P., Galbraith, M., & Patursson, Ø. (2015). Abundance and distribution of planktonic _Lepeophtheirus salmonis_ and _Caligus elongatus_ in a fish farming region in the Faroe Islands. _Aquaculture Environment Interactions_, 7(1), 15–27. https://doi.org/10.3354/aei00134

Aas, T. S., Ytrestøyl, T., & Åsgård, J. E. (2019). Utilization of feed resources in the production of Atlantic salmon (_Salmo salar_) in Norway: An update for 2016. _Aquaculture Reports_, 15, 100216. https://doi.org/10.1016/j.aqrep.2019.100216

Abolofia, J., Asche, F., & Wilen, J. E. (2017). The cost of lice: Quantifying the impacts of parasitic sea lice on farmed salmon. _Marine Resource Economics_, 32(3), 329–349. https://doi.org/10.1086/691981

Andrade-Eiroa, Á., Canle, M., & Cerdá, V. (2013). Environmental applications of excitation-emission spectrofluorimetry: An in-depth review II. _Applied Spectroscopy Reviews_, 48(2), 77–141. https://doi.org/10.1080/05704928.2012.692105

Bjørndal, T., & Tusvik, A. (2019). Economic analysis of land based farming of salmon. _Aquaculture Economics & Management_, 23(4), 449–475. https://doi.org/10.1080/13657305.2019.1654558

Boxhall, G. A. (1998). Preface to the themed discussion on 'Mating biology of copepod crustaceans'. _Philosophical Transactions of the Royal Society B: Biological Sciences_, 353(1369), 669–670.

Brooker, A. J., Skern-Mauritzen, R., & Bron, J. E. (2018). Production, mortality, and infectivity of planktonic larval sea lice, _Lepeophtheirus salmonis_ (Krøyer, 1837): Current knowledge and implications for epidemiological modelling. _ICES Journal of Marine Science_, 75(4), 1214–1234. https://doi.org/10.1093/icesjms/fsy015

Buesa, R. J. (2008). Histology without formalin? _Annals of Diagnostic Pathology_, 12(6), 387–396. https://doi.org/10.1016/j.anndiagpath.2008.07.004

Bui et al (2020). _Finding the needle in a haystack: comparison of enumeration methods for a rare parasitic copepod species in plankton samples._ [Manuscript submitted for publication].

Byrne, A. A., Pearce, C. M., Cross, S. F., Jones, S. R., Robinson, S. M., Hutchinson, M. J., Miller, M. R., Haddad, C. A., & Johnson, D. L. (2018). Planktonic and parasitic stages of sea lice (_Lepeophtheirus salmonis_ and _Caligus clemensi_) at a commercial Atlantic salmon (_Salmo salar_) farm in British Columbia, Canada. _Aquaculture_, 486, 130–138. https://doi.org/10.1016/j.aquaculture.2017.12.009

Carstea, E. M., Bridgeman, J., Baker, A., & Reynolds, D. M. (2016). Fluorescence spectroscopy for wastewater monitoring: A review. _Water Research_, 95, 205–219. https://doi.org/10.1016/j.watres.2016.03.021

Coble, P. G. (1996). Characterization of marine and terrestrial DOM in seawater using excitation-emission matrix spectroscopy. _Marine Chemistry_, 51(4), 325–346.

Costello, M. J. (2009a). The global economic cost of sea lice to the salmonid farming industry. _Journal of Fish Diseases_, 32(1), 115–118. https://doi.org/10.1111/j.1365-2761.2008.01011.x

Costello, M. J. (2009b). How sea lice from salmon farms may cause wild salmonid declines in Europe and North America and be a threat to fishes elsewhere. _Proceedings of the Royal Society B: Biological Sciences_, 276(1672), 3385–3394. https://doi.org/10.1098/rspb.2009.0771

Dalvin, S., Frost, P., Biering, E., Hamre, L. A., Eichner, C., Krossøy, B., & Nilsen, F. (2009). Functional characterisation of the maternal yolk-associated protein (LsYAP) utilising systemic RNA interference in the salmon louse (_Lepeophtheirus salmonis_)(Crustacea: Copepoda). _International Journal for Parasitology_, 39(13), 1407–1415. https://doi.org/10.1016/j.ijpara.2009.04.004

Dalvin, S., Frost, P., Loeffen, P., Skern-Mauritzen, R., Baban, J., Rønnestad, I., & Nilsen, F. (2011). Characterisation of two vitellogenins in the salmon louse _Lepeophtheirus salmonis_: Molecular, functional and evolutional analysis. _Diseases of Aquatic Organisms_, 94(3), 211–224. https://doi.org/10.3354/dao02331

Dapson, R. W. (2010). Mechanisms of action and proper use of common fixatives. In C. R. Taylor, & S. R. Shi (Eds.), _Antigen retrieval immunohistochemistry based research and diagnostics_. John Wiley & Sons, Incorporated, ProQuest Ebook Central.

Davidsen, J. G., Knudsen, R., Power, M., Sjursen, A. D., Rønning, L., Hårsaker, K., Næsje, T. F., & Arnekleiv, J. V. (2017). Trophic niche similarity among sea trout _Salmo trutta_ in central Norway investigated using different time-integrated trophic tracers. _Aquatic Biology_, 26, 217–227. https://doi.org/10.3354/ab00689

Falkenhaug, T., Tande, K., & Timonin, A. (1997). Spatio-temporal patterns in the copepod community in Malangen, Northern Norway. _Journal of Plankton Research_, 19(4), 449–468. https://doi.org/10.1093/plankt/19.4.449

FAO. (2020). Fisheries Global Information System (FAO-FIGIS) - Web site. _Fisheries Global Information System (FIGIS)_. FI Institutional Websites. In FAO Fisheries Division [online]. Rome. Updated. [Cited 10 September 2020].

Fjørtoft, H. B., Nilsen, F., Besnier, F., Stene, A., Bjørn, P. A., Tveten, A. K., Aspehaug, V. T., Finstad, B., & Glover, K. A. (2019). Salmon lice sampled from wild Atlantic salmon and sea trout throughout Norway display high frequencies of the genotype associated with pyrethroid resistance. _Aquaculture Environment Interactions_, 11, 459–468. https://doi.org/10.3354/aei00322

Fordyce, M. (2017). _An improved method for the visualization of salmon louse_ Lepeophtheirus salmonis _copepodids from plankton samples by fluorescence stereomicroscopy._ Poster presented at: International Conference on Diseases of Fish and Shellfish. 2017 Sep 4–8. Belfast, Northern Ireland.

Fox, C. H., Johnson, F. B., Whiting, J., & Roller, P. P. (1985). Formaldehyde fixation. _Journal of Histochemistry & Cytochemistry_, 33(8), 845–853. https://doi.org/10.1177/33.8.3894502

Glover, K. A., Stølen, Å. B., Messmer, A., Koop, B. F., Torrissen, O., & Nilsen, F. (2011). Population genetic structure of the parasitic copepod _Lepeophtheirus salmonis_ throughout the Atlantic. _Marine Ecology Progress Series_, 427, 161–172. https://doi.org/10.3354/meps09045

Gravil, H. R. (1996). _Studies on the biology and ecology of the free swimming larval stages of Lepeophtheirus salmonis (Kroyer, 1838) and Caligus elongatus Nordmann, 1832 (Copepoda: Caligidae)._ (Unpublished Doctoral dissertation). University of Stirling.

Gundersen, K. R. (1953). Zooplankton investigations in some fjords in Western Norway during 1950–1951. _Fiskeridirektoratets Skrifter_, 10(6), 1–54.

Hamre, L. A., Eichner, C., Caipang, C. M. A., Dalvin, S. T., Bron, J. E., Nilsen, F., Boxshall, G., & Skern-Mauritzen, R. (2013). The Salmon Louse _Lepeophtheirus salmonis_ (Copepoda: _Caligidae_) life cycle has only two chalimus stages. _PLoS One_, 8(9), e73539. https://doi.org/10.1371/journal.pone.0073539

Hamre, L. A., Glover, K. A., & Nilsen, F. (2009). Establishment and characterisation of salmon louse (_Lepeophtheirus salmonis_ (Krøyer 1837)) laboratory strains. _Parasitology International_, 58(4), 451–460. https://doi.org/10.1016/j.parint.2009.08.009

Heuch, P. A., Bjørn, P. A., Finstad, B., Holst, J. C., Asplin, L., & Nilsen, F. (2005). A review of the Norwegian 'National Action Plan Against Salmon Lice on Salmonids': The effect on wild salmonids. *Aquaculture*, *246*(1–4), 79–92. https://doi.org/10.1016/j.aquaculture.2004.12.027

Hudson, N., Baker, A., & Reynolds, D. (2007). Fluorescence analysis of dissolved organic matter in natural, waste and polluted waters—A review. *River Research and Applications*, *23*(6), 631–649. https://doi.org/10.1002/rra.1005

Kristoffersen, A. B., Qviller, L., Helgesen, K. O., Vollset, K. W., Viljugrein, H., & Jansen, P. A. (2018). Quantitative risk assessment of salmon louse-induced mortality of seaward-migrating post-smolt Atlantic salmon. *Epidemics*, *23*, 19–33. https://doi.org/10.1016/j.epidem.2017.11.001

Krkosek, M., Ford, J. S., Morton, A., Lele, S., Myers, R. A., & Lewis, M. A. (2007). Declining wild salmon populations in relation to parasites from farm salmon. *Science*, *318*(5857), 1772–1775. https://doi.org/10.1126/science.1148744

Krkošek, M., Lewis, M. A., & Volpe, J. P. (2005). Transmission dynamics of parasitic sea lice from farm to wild salmon. *Proceedings of the Royal Society B: Biological Sciences*, *272*(1564), 689–696. https://doi.org/10.1098/rspb.2004.3027

Krkošek, M., Revie, C. W., Gargan, P. G., Skilbrei, O. T., Finstad, B., & Todd, C. D. (2013). Impact of parasites on salmon recruitment in the Northeast Atlantic Ocean. *Proceedings of the Royal Society B: Biological Sciences*, *280*(1750), 20122359. https://doi.org/10.1098/rspb.2012.2359.

Lakowicz, J. R. (Ed.). (2013). *Principles of fluorescence spectroscopy*. Springer Science & Business Media.

Murphy, K. R., Stedmon, C. A., Graeber, D., & Bro, R. (2013). Fluorescence spectroscopy and multi-way techniques. PARAFAC. *Analytical Methods*, *5*(23), 6557–6566. https://doi.org/10.1039/C3AY41160E

Myksvoll, M. S., Sandvik, A. D., Albretsen, J., Asplin, L., Johnsen, I. A., Karlsen, Ø., Kristensen, N. M., Melsom, A., Skardhamar, J., & Ådlandsvik, B. (2018). Evaluation of a national operational salmon lice monitoring system—From physics to fish. *PLoS One*, *13*(7), e0201338. https://doi.org/10.1371/journal.pone.0201338

Myksvoll, M. S., Sandvik, A. D., Johnsen, I. A., Skarðhamar, J., & Albretsen, J. (2020). Impact of variable physical conditions and future increased aquaculture production on lice infestation pressure and its sustainability in Norway. *Aquaculture Environment Interactions*, *12*, 193–204. https://doi.org/10.3354/aei00359

Nelson, E. J., Robinson, S. M. C., Feindel, N., Sterling, A., Byrne, A., & Pee Ang, K. (2017). Horizontal and vertical distribution of sea lice larvae (*Lepeophtheirus salmonis*) in and around salmon farms in the Bay of Fundy. *Canada. Journal of Fish Diseases*, *41*(6), 885–899. https://doi.org/10.1111/jfd.12692

Nielsen, J. H., Pedersen, C., Kiørboe, T., Nikolajsen, T., Brydegaard, M., & Rodrigo, P. J. (2019). Investigation of autofluorescence in zooplankton for use in classification of larval salmon lice. *Applied Optics*, *58*(26), 7022–7027. https://doi.org/10.1364/AO.58.007022

Nielsen, T., & Andersen, C. (2002). Plankton community structure and production along a freshwater-influenced Norwegian fjord system. *Marine Biology*, *141*(4), 707–724. https://doi.org/10.1007/s00227-002-0868-8

Nilsen, M. K. (2016). *Sampling strategies, distribution and concentration of planktonic salmon lice copepods in the Outer Hardangerfjord and the Altafjord* (Unpublished Master's thesis), UiT Norges arktiske universitet. https://hdl.handle.net/10037/10003

O'Brien, T. D., Wiebe, P. H., & Falkenhaug, T. (Eds). (2013). *ICES zooplankton status report 2010/2011*. International Council for the Exploration of the Sea.

Penston, M. J., McBeath, A. J., & Millar, C. P. (2011). Densities of planktonic *Lepeophtheirus salmonis* before and after an Atlantic salmon farm relocation. *Aquaculture Environment Interactions*, *1*(3), 225–232. https://doi.org/10.3354/aei00022

R Core Team. (2018). *R: A language and environment for statistical computing*. R Foundation for Statistical Computing, Vienna, Austria. https://www.R-project.org/

Richardson, T. L., Lawrenz, E., Pinckney, J. L., Guajardo, R. C., Walker, E. A., Paerl, H. W., & MacIntyre, H. L. (2010). Spectral fluorometric characterization of phytoplankton community composition using the Algae Online Analyser®. *Water Research*, *44*(8), 2461–2472. https://doi.org/10.1016/j.watres.2010.01.012

SádeCká, J., & TóThoVá, J. (2007). Fluorescence spectroscopy and chemometrics in the food classification-a review. *Czech Journal of Food Sciences*, *25*(4), 159–173.

Salama, N. K. G., Collins, C. M., Fraser, J. G., Dunn, J., Pert, C. C., Murray, A. G., & Rabe, B. (2013). Development and assessment of a biophysical dispersal model for sea lice. *Journal of Fish Diseases*, *36*(3), 323–337. https://doi.org/10.1111/jfd.12065

Samsing, F., Oppedal, F., Dalvin, S., Johnsen, I., Vågseth, T., & Dempster, T. (2016). Salmon lice (*Lepeophtheirus salmonis*) development times, body size, and reproductive outputs follow universal models of temperature dependence. *Canadian Journal of Fisheries and Aquatic Sciences*, *73*(12), 1841–1851. https://doi.org/10.1139/cjfas-2016-0050

Sandvik, A. D., Bjørn, P. A., Ådlandsvik, B., Asplin, L., Skarðhamar, J., Johnsen, I. A., Myksvoll, M., & Skogen, M. D. (2016). Toward a model-based prediction system for salmon lice infestation pressure. *Aquaculture Environment Interactions*, *8*, 527–542. https://doi.org/10.3354/aei00193

Sandvik, A. D., Johnsen, I. A., Myksvoll, M. S., Sævik, P. N., & Skogen, M. D. (2020). Prediction of the salmon lice infestation pressure in a Norwegian fjord. *ICES Journal of Marine Science*, *77*(2), 746–756. https://doi.org/10.1093/icesjms/fsz256

Schram, T. A. (2004). Practical identification of pelagic sea lice larvae. *Journal of the Marine Biological Association of the United Kingdom*, *84*(1), 103–110. https://doi.org/10.1017/S0025315404008963h

Skarðhamar, J., Fagerli, M. N., Reigstad, M., Sandvik, A. D., & Bjørn, P. A. (2019). Sampling planktonic salmon lice in Norwegian fjords. *Aquaculture Environment Interactions*, *11*, 701–715. https://doi.org/10.3354/aei00342

Skern-Mauritzen, R., Sissener, N. H., Sandvik, A. D., Meier, S., Sævik, P. N., Skogen, M. D., Vågseth, T., Dalvin, S., Skern-Mauritzen, M., & Bui, S. (2020). Parasite development affect dispersal dynamics; infectivity, activity and energetic status in cohorts of salmon louse copepodids. *Journal of Experimental Marine Biology and Ecology*, *530*, 151429. https://doi.org/10.1016/j.jembe.2020.151429

Skern-Mauritzen, R., Torrissen, O., & Glover, K. A. (2014). Pacific and Atlantic Lepeophtheirus salmonis (Krøyer, 1838) are allopatric subspecies: Lepeophtheirus salmonis salmonis and L. salmonis oncorhynchi subspecies novo. *BMC Genetics*, *15*(1), 32. https://doi.org/10.1186/1471-2156-15-32

Stien, A., Bjørn, I. A., Heuch, P. A., & Elston, D. A. (2005). Population dynamics of salmon lice *Lepeophtheirus salmonis* on Atlantic salmon and sea trout. *Marine Ecology Progress Series*, *290*, 263–275.

Taranger, G. L., Karlsen, Ø., Bannister, R. J., Glover, K. A., Husa, V., Karlsbakk, E., Kvamme, B. O., Boxaspen, K. K., Bjørn, P. A., Finstad, B., Madhun, A. S., Morton, H. C., & Svåsand, T. (2014). Risk assessment of the environmental impact of Norwegian Atlantic salmon farming. *ICES Journal of Marine Science*, *72*(3), 997–1021. https://doi.org/10.1093/icesjms/fsu132

Thompson, C. R., Bron, J., Bui, S., Dalvin, S., Fordyce, M. J., Furmanek, T., á Norði, G., & Skern-Mauritzen, R. (2020). Illuminating the planktonic stages of salmon lice: a unique fluorescence signal for rapid identification of a rare copepod in zooplankton assemblages. [Data set] . Zendo. https://doi.org/10.5281/zenodo.4157041

Thompson, C. R., Fields, D. M., Bjelland, R. M., Chan, V. B., Durif, C. M., Mount, A., Runge, J. A., Shema, S. D., Skiftesvik, A. B., & Browman, H.

I. (2019). The planktonic stages of the salmon louse (*Lepeophtheirus salmonis*) are tolerant of end-of-century $pCO_2$ concentrations. *PeerJ, 7*, e7810. https://doi.org/10.7717/peerj.7810

Thorstad, E. B., Todd, C. D., Uglem, I., Bjørn, P. A., Gargan, P. G., Vollset, K. W., Halttunen, E., Kålås, S., Berg, M., & Finstad, B. (2015). Effects of salmon lice *Lepeophtheirus salmonis* on wild sea trout *Salmo trutta*—a literature review. *Aquaculture Environment Interactions, 7*(2), 91–113. https://doi.org/10.3354/aei00142

Tocher, J. A., Dick, J. R., Bron, J. E., Shinn, A. P., & Tocher, D. R. (2010). Lipid and fatty acid composition of parasitic caligid copepods belonging to the genus *Lepeophtheirus*. *Comparative Biochemistry and Physiology Part B: Biochemistry and Molecular Biology, 156*(2), 107–114. https://doi.org/10.1016/j.cbpb.2010.02.010

Torrissen, O., Jones, S., Asche, F., Guttormsen, A., Skilbrei, O. T., Nilsen, F., Horsberg, T. E., & Jackson, D. (2013). Salmon lice–impact on wild salmonids and salmon aquaculture. *Journal of Fish Diseases, 36*(3), 171–194. https://doi.org/10.1111/jfd.12061

Vollset, K. W., Dohoo, I., Karlsen, Ø., Halttunen, E., Kvamme, B. O., Finstad, B., Wennevik, V., Diserud, O. H., Bateman, A., Friedland, K. D., Mahlum, S., Jørgensen, C., Qviller, L., Krkošek, M., Åtland, Å., & Barlaup, B. T. (2018). Disentangling the role of sea lice on the marine survival of Atlantic salmon. *ICES Journal of Marine Science, 75*(1), 50–60. https://doi.org/10.1093/icesjms/fsx104

## SUPPORTING INFORMATION

Additional supporting information may be found online in the Supporting Information section.

**How to cite this article:** Thompson CRS, Bron JE, Bui S, et al. Illuminating the planktonic stages of salmon lice: A unique fluorescence signal for rapid identification of a rare copepod in zooplankton assemblages. *J Fish Dis*. 2021;00:1–17. https://doi.org/10.1111/jfd.13345